International Journal of Modern Engineering Research (IJMER)
www.ijmer.com Vol.2, Issue.2, Mar-Apr 2012 pp-025-042 ISSN: 2249-6645

Study of the wear and friction behavior of immiscible as cast-Al-Sn/Graphite composite

S.Srivastava[1*], S. Mohan[2], Yogesh Srivastava[1] and Aman J. Shukla[3]
[1]Materials Science & Metallurgical Engineering
[1] Maulana Azad National Institute of Technology, Bhopal M.P. (India)-462051
[2]Institute of Technology, Banaras Hindu University, Varanasi-221005
[3]Research & Technology Development Centre
Sharda University, G. Noida U.P. (India)-201306

Abstract:
In this paper we investigate the tribological properties of Al-Sn-based alloy with different amount of graphite at different normal loads and sliding speed. A modified impeller mixing coupled with chill casting technique was used for the preparation of immiscible alloys. In this paper Al-Sn binary alloys was chosen for this study. This binary system shows the miscibility gap at different concentration and temperature. Graphite was chosen as reinforcing element which was reinforced in the Al-Sn matrix. The graphite content in the composite varied from 1.6 to 8.4 wt%. The presence of graphite in the matrix not only improves the mechanical properties but also improve the tribological properties due to lubricating action. The ductility of composite materials showed the adverse effect with increase of the graphite content in the matrix. Pin-on-disc sliding wear tests were conducted in an ambient condition to examine the tribological behavior of the aluminum-based graphite composite. The experiment was commenced at different sliding distance, speed and using normal load. Having finished the tests, the weight losses of the specimen were measured, wear and friction characteristics were calculated with respect to time, depth of wear track, sliding speed and bearing load. Friction coefficient and wear volume have shown large sensitivity to the applied normal load and the testing time (or sliding distance). The XRD and SEM analysis were used to analyze the wear debris and track.

Key words: Aluminum alloy, Friction coefficient, Pin-on-Disc, SEM, Sliding velocity, Tribometer, Wear, and XRD.

1. Introduction

Aluminum alloys and other lightweight materials have growing applications in the automotive industry, with respect to reducing the fuel utilization and shielding the environment, where they can successfully reinstate steel and cast iron parts. There are a number of elements which have a limited solubility in the aluminum matrix. Therefore they exhibit two immiscible liquid phases within a certain temperature range. However, the different densities of these liquid phases lead, to the formation of two different layers. This prevents the homogeneous distribution of particles in a matrix using simple and inexpensive casting processes. The development of immiscible alloys has been largely constrained by the conventional equilibrium processing, which generally results in gross segregation due to the wide miscibility gap, and high disparity in the densities and melting temperatures between the immiscible elements [1, 2]. The idea is to obtain aluminum matrix with finely distributed particles of *e.g*. indium, bismuth or lead as a soft phase or iron, nickel or cobalt as a hard phase with lubricating function. However this is still far from the practical application because the miscibility phenomenon poses problems during solidification [3-5]. A miscible gap in the liquid state is found in metal-metal systems such as Al-Bi, Al-Pb, Al-In, Al-Sn, Cu-Pb, and Zn-Pb, Ga-Pb etc. For this study Al-Sn was selected as basic materials in which small amount of the graphite was added for improving the wear and seizure properties of the materials. A typical equilibrium phase diagram is shown in Fig.1. The solid solubility is of the order of 0.10% Sn at approximately 900. ^{0}K, decreasing to reach a probable value of 0.05-0.07% Sn at eutectic temperature, and much smaller values at lower temperatures. The density increased is approximately 0.06% for every 0.1% Sn added. Liquid gas surface tension and ratio solid-liquid /solid-solid surface tension decreases, and this affect the shape of phase. Fluidity is greatly reduced, and electric conductivity is decreased. There is practically no change in hardness, strength or elongation of commercial aluminium, high purity aluminium is slightly strengthened. Strength and especially elongation drop rapidly with temperature at 500^{o}K the strength of a 10% tin alloy is halved and the elongation has dropped from 60% at room temperature to less than 5% at 900^{o}K the alloy are brittle. Plastic deformation to break the tin network, followed by annealing to spheroidized the tin improve the properties [6].

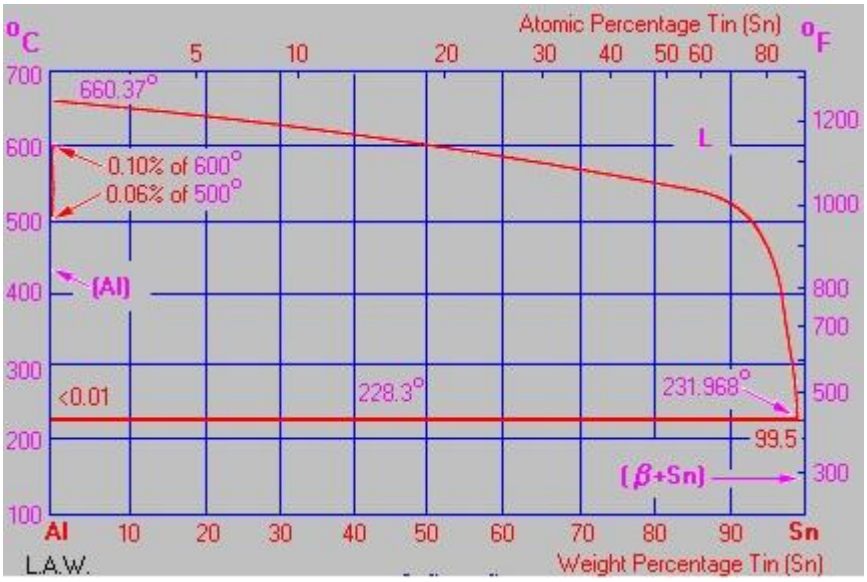

Fig. 1. Phase diagram of Al-Sn

With solid lubricant particle like graphite or MoS_2 dispersion in the matrix of aluminum alloy this material exhibits good potential for resistant to wear and consequently becomes more suitable for tribological applications [7-9].Considerable efforts have been put into incorporating lubricating particles in aluminum alloy matrices to improve resistant to wear. Earlier researcher [9-12] has reported graphite as a suitable solid lubricating material for the preferred applications. Aluminum alloy–Graphite particulate composite exhibits its potential to act as a self lubricating material with improved resistance to wear, machinability, delayed on set of severe wear and seizure. P.R. Gibson et al [13, 14] and S. Das et al [15] investigated that a solid lubricating film can be formed on the wearing surface with addition of graphite particulate in the aluminum alloy. It helps in reducing the friction coefficient and to increase the anti seizing quality and also improve tribological behavior of the base alloy. Jha et al [7] have observed that the porosity encountered during the production of aluminum-graphite composite material embrittles the material with crack nucleation and reduction in fracture toughness and elongation of the matrix alloy leading to increased wear. However addition of appropriate level of graphite particulate can reduce it. Also at increased sliding speeds the wear rate decreases with addition of graphite content [16-20].

The present article aims to contribute to a better understanding of the interrelation between presence of the graphite particles in the matrix and the corresponding mechanical properties and wear behavior. In the present work, Al-Sn composite with different amount of graphite are being produced by liquid metallurgical route. Experimental quantitative expressions, which correlate the ultimate tensile strength (UTS), yield tensile strength, elongation, wear volume and frictional coefficients to the presence of graphite in the matrix, have been determined.

2. Experimental investigation

2. 1 Selection of materials

Commercially pure aluminium (99.8%) and tin-metal were selected for the preparation of Al-Sn composites with different content of graphite.

2.2 Procedure for preparation

The experimental set-up used for mixing and casting of composites is shown in Fig 2. It comprises of a cylindrical sillimanite crucible of 150mm diameter and 250mm depth with attachment of four baffles to its sidewalls for proper dispersion of second phase in melt during stirring. The crucible was placed in an electric heated muffle furnace. It was also equipped with a bottom pouring attachment, which could be closed or opened by graphite stopper with a lever system. A steel mould was placed beneath the furnace to cast the molten metal. In the top cover suitable opening was provided to charge materials and insert thermocouples. The temperature of the furnace could be controlled with an accuracy of about $\pm 5^0$C. Metallic bath temperature was measured continuously by chromel/alumel thermocouple. The agitator system could be raised or lowered with the help of the hanger and steel frame structure. After adjusting the mixer in a central position and required height from the bottom of the crucible, the motor was bolted and locked while mixing of melt. Three-blade impeller was used for effective mixing. This design provides very high rates of shear and only axial and radial flow currents are utilized for mixing without any significant vortex formation due to the presence of baffles. The Al-Sn-graphite composites were prepared employing liquid metallurgical route. The required

amount of commercial pure aluminum was charged into the crucible and aluminum was heated to a temperature 200^0C above its melting point i.e. 662^0C. A mechanical stirrer was inserted into the melt, and agitation was started at a speed of 35 s^{-1}. The 50-µm-size electrolytic grade graphite powder was charged into the melt during stirring and the addition of the particulate into the melt was facilitated by vortex created by stirring action. Mixing was done for a period of 60 seconds. The emulsion was poured into the chilled cylindrical mould placed beneath the crucible. The same procedure was adopted for different compositions. Cylindrical casting of length 20cm and dia.2cm were obtained.

2.3 Evaluation of as-cast Properties of the Composite

The wet chemical analysis was used to determine the percentage of iron in the bulk .The metallographic specimens were prepared using standard technique and studied under SEM for different feature present. The densities of the composite were determined using Archimedes' principle by weighing in water and air. The hardness of the entire composite was measured using a Vickers hardness testing machine. The hardness of the entire composite was measured using a Vickers hardness testing machine. The hardness was measured using Vickers hardness instrument Leitz Welzlar at a load of 5Kg. At least 3 indentations have been taken for each point. Tensile testing of all the Al-alloy-graphite composite was performed stress along with percentage elongation and reductions in area were computed from the results.

2.4 Wear test

Pin-on-disc machine was used for evaluating the wear properties under dry sliding condition. The cylindrical test pin of 8mm diameter and 40mm length were used against a hardened steel disc of 120 mm diameter. Wear tests were conducted with variable applied pressure $3.9x10^{-1}$ Mpa and a sliding speed of 0.5 m/s with a constant sliding distance of 10000 meters. Wear test were also conducted with selected varying speeds and sliding distance ranging up to 1000 meters. The initial weight of the specimen was determined in a digital balance with a precision of ± 0.1 mg. The pin was kept pressed against a rotating steel disc of hardness 58 HRc under loaded condition. The frictional traction en-counted by the pin in sliding is measured by a PC based data logging system. On completion of the running through the required sliding distance the specimen pins were cleaned with acetone, dried and their weight were again determined for ascertaining the weight loss. Wear debris were analyzed by XRD.

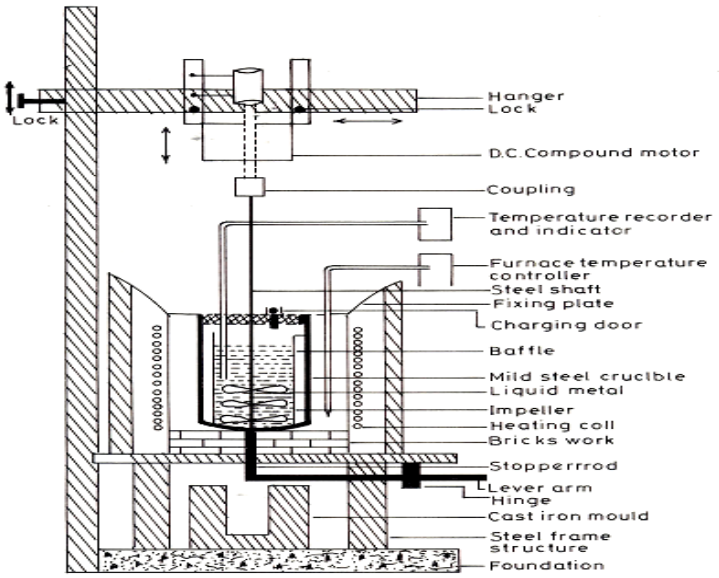

Fig 2.-Schematic diagram of casting set-up

3. Result and Discussion

3.1 Physical investigation

The liquid metallurgy methods were used to synthesize the composite materials with different amount of the graphite content in the matrix. The theoretical density of the composite materials varies from 2.88 g/c.c to 2.84 g/cc with graphite content. But the experimental density of the composite materials was found to vary from 2.72 g/cc to 2.70 g/cc along with porosity varies from 5.2 % to 4.9 %. The XRD methods were used to investigate the different phase/element present in the prepared composite materials. Fig 3 shows the XRD pattern of Al-6.3%Sn-3.4%Gr composite. The XRD scanning from 10°-80° shows the lines (200) , (101),(400), (220), (511), (211) for tin (111), (101)(110) (222) (112) for graphite, small peak of Al_2O_3 {(110) and

(005)}, along with aluminum peak aluminum {(111) (200), etc} at 2θ = 30.62°, 32.09°, 43.9°, 44.9^0, 62.6° for tin, 26.7, 43.5, 46.4 and 56.68 for graphite 15.45, 18.99^o for alumina, 38.86°, for aluminum respectively.

3.2 Study of the mechanical properties

The resistance to indentation or scratch is termed as hardness. Among various instruments for measurement of hardness, Brinell's, Rockwell's and Vickers's hardness testers are significant. Theoretically, the rule of mixture of the type $H_c=v_rH_r+v_mH_m$ (suffixes 'c', 'r', and 'm' stand for composite, reinforcement and matrix respectively and *v* and H stand for volume fraction and hardness respectively) is valid for composites materials which helps in approximating the hardness values. Among the variants of reinforcements, the low aspect ratio particle reinforcements are of much significant in imparting the hardness of the material in which they are dispersed. Table 1 shows a comparison of the mechanical properties of Al-Sn/graphite composite samples produced by the liquid metallurgy methods. Fig.4 shows the variation of mechanical properties with the graphite content in the Al-Sn alloys. It is observed that the hardness of the composite materials decrease with increasing the graphite content in the matrix. Graphite is a very brittle materials and it is responsible factor for decreasing the hardness of the materials.

The uniform distribution and the nature of the interfacial bonding between graphite particles and matrix have an important relationship on the mechanical properties of a composite material. It has been suggested that graphite particles, being very weak compared to the aluminum matrix, may be treated as non-load-bearing constituents **[**21**]**. With a view to extending their applications to structural components, these materials should have a good combination of strength and ductility. The Al-Sn/graphite composites with different graphite content show an increase in the tensile elongation together with an increase in the ultimate tensile strength of the material, resulting from the better dispersion of the particles. The magnitudes of these increases are observed to average approximately 18%. A strong bond between the reinforcement and matrix helps in the load transfer from the latter to the former. As a result, fracture takes place in the composite via the reinforcement and not along the interface [22, 23**]**. Although the graphite is a non-load bearing constituent, a strong particle/matrix interface helps graphite particles embed themselves into the matrix properly, improving the fracture resistance.

3.3 Wear study

3.3.1 Effect of sliding distance and load

The variation of bulk wear with sliding distance was studied at different combinations of loads and sliding velocities. Almost a linear relationship in bulk wear and sliding distance i.e. steady state wear is observed after an initial running-in period of 500–1000 m in almost all the cases irrespective of load or sliding velocity used.

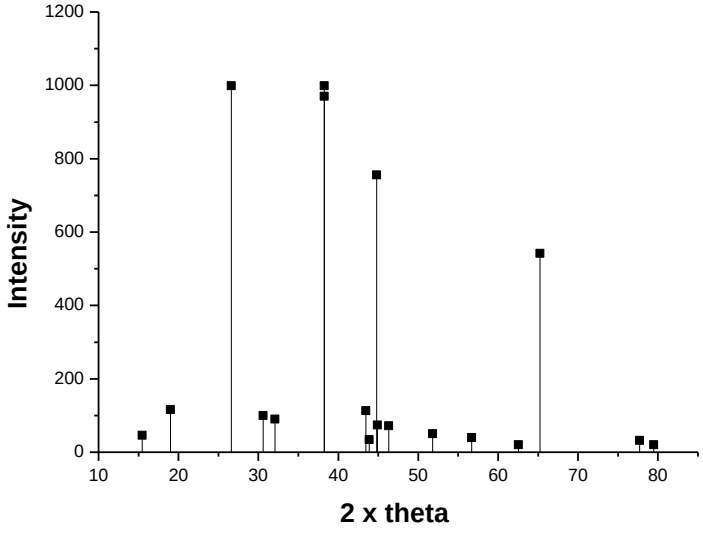

Fig 3. XRD graph of Al-6.3%Sn-3.4%Gr composite

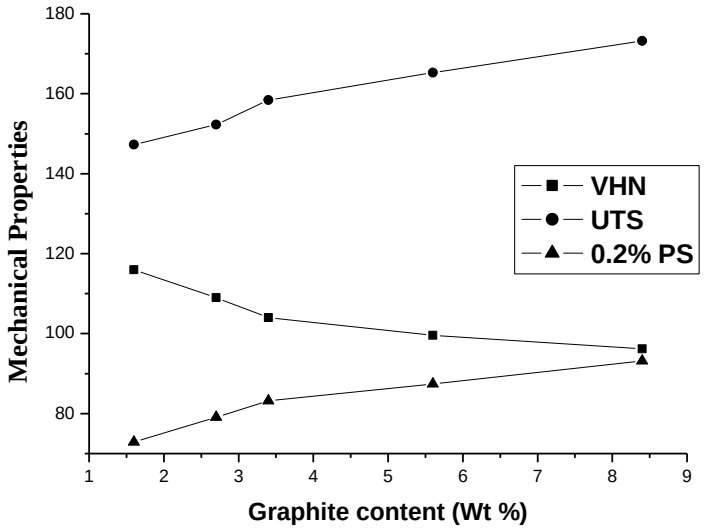

Fig 4. Variation of hardness with varying graphite content

Table 1- Mechanical properties of the Al-Sn/ Graphite composite

S.No.	Composite	VHN	UTS (MPa)	0.2%PS(MPa)	% elongation
1	Al-6.3%Sn-1.6%Gr	116	147.3	72.9	16.3
2	Al-6.3%Sn-2.7%Gr	109	152.3	79.1	16.9
3	Al-6.3%Sn-3.4%Gr	104	158.4	83.2	17.3
4	Al-6.3%Sn-5.6%Gr	99.6	165.3	87.4	18.1
5	Al-6.3%Sn-8.4%Gr	96.2	173.2	93.2	19.3

Fig. 5 shows results for a test conducted at 2 kg load and 0.5m/s sliding velocity. In running in period, the Al-Sn/graphite composite shows large wear rates. The relation found here is in accordance with the pattern for most metallic materials derived theoretically as well as observed experimentally [18,19]. But irrespective of variables used, bulk wear is large with large graphite content in Al-Sn/graphite composite. The self-lubricated role of graphite reinforcing particles was significant in dry sliding conditions, as well as in conditions of lubricated sliding. The free graphite particles are released from the composite material during dry sliding of mating surfaces form a lubricant film at the interface. Fig.6 shows the variation of rise in temperature of the test specimen during experiment with sliding distance. The maximum rise in temperature is found in Al-6.3%Sn-1.6%Gr and minimum in Al-6.3%Sn-8.4%Gr. This type of the behavior can be explained on the basis of thermal conductivity. Al-6.3%Sn-1.6%Gr shows less conductivity as Al-6.3%Sn-8.4%Gr. Fig. 7 shows the SEM micrographs of wear tracks of Al-Sn/graphite composites (Al-6.3%Sn-3.4%Gr**)** for 2 kg applied load and 0.5 m/s sliding velocity at 10,000 m sliding distances. This micrograph was taken at the higher magnification. This figure is clearly revealed the presence of the oxide layer which might be adhered on the rubbing surface.

3.3.2 Effect of applied load

The studies conducted to see the effect of applied load on wear rate revealed that wear rate increases continuously with load in a linear manner irrespective of the sliding velocity used as it is evident from Fig. 8 for a particular velocity. But in all the cases wear rate first decreases with increase in graphite content for all combinations of loads and sliding velocities used in the present investigation and then increase with increase the graphite content. Corresponding temperature curve shown in Fig.9, clearly reveal that temperature continuously increases with increase in load but with increase in iron percentage in composite a decrease in temperature rise is observed

which is indicative of larger heat dissipation capability of iron.

Fig. 8 shows the variation of temperature and micro hardness of the test specimen with the variation of load. With increase the load on the test specimen, the composite material bears maximum rise in temperature. The materials at the contacting surface on the pin-on-disc become soften, which is responsible factor for decreasing the micro hardness of the contacting surface. As expected, the high wear resistance of Al-graphite composites is primarily to due to the presence of graphite particles which act as a solid lubricant.

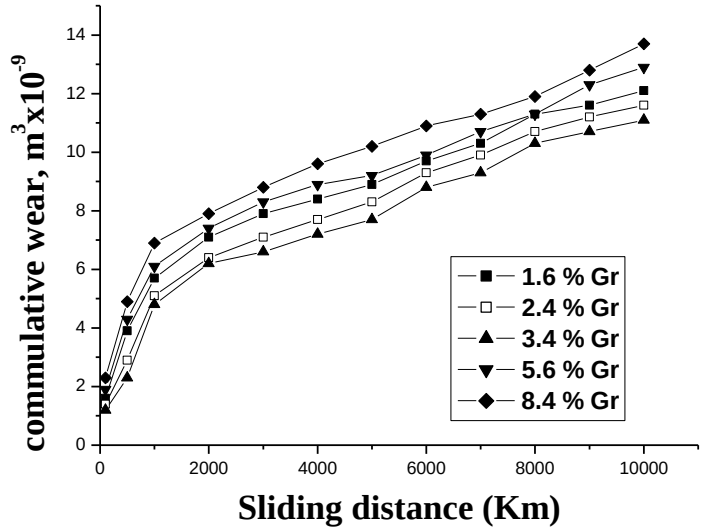

Fig 5. Variation of bulk wear with sliding distance at 2 kg load and 0.5 m/s sliding velocity for as-cast Al-Sn/graphite composites.

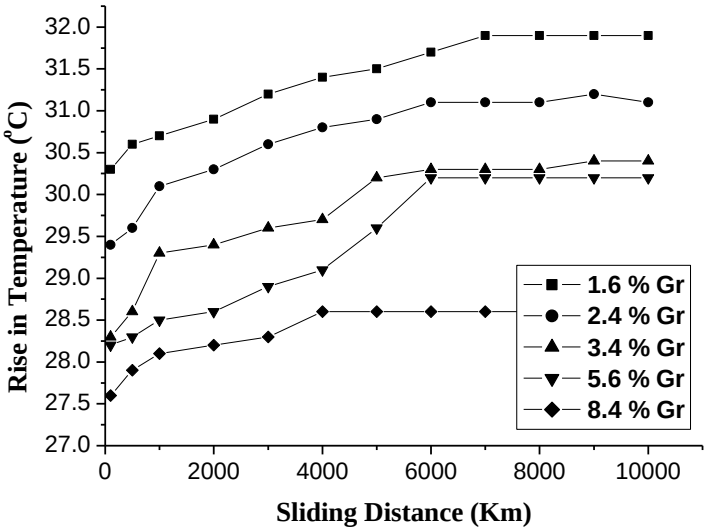

Fig 6. Variation of rise in temperature of the test specimen with sliding distance at 2 kg load and 0.5 m/s sliding velocity for as-cast Al-Sn/graphite composites.

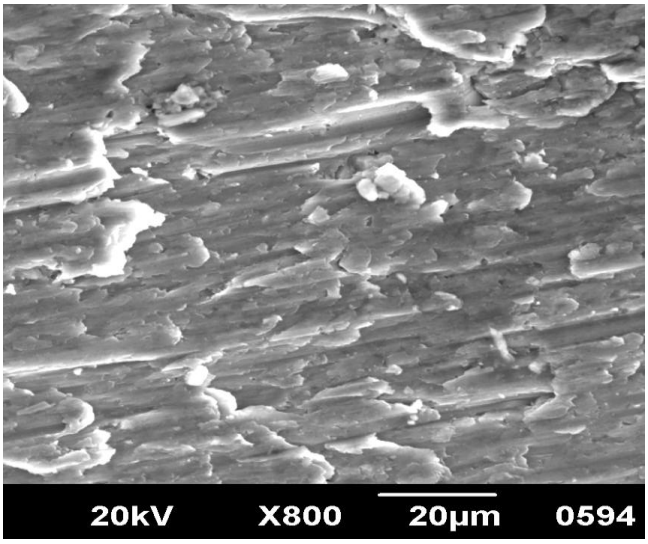

Fig 7. SEM micrographs of wear tracks of Al-Sn/graphite composites (Al-6.3%Sn-3.4%Gr) for 2 kg applied load and 0.5 m/s sliding velocity at 10,000 m sliding distances.

Fig. 11 shows the SEM micrographs of wear tracks of Al-Sn/graphite composites (Al-6.3%Sn-3.4%Gr) at the higher magnification for 2 kg applied load and 0.5 m/s sliding velocity at 3000 m sliding distances. The oxides layer with small amount of the graphite particles are adhered on the material surface. Fig. 12 a and b : SEM micrographs of wear tracks of Al-Sn/graphite composites (Al-6.3%Sn-3.4%Gr) for 15 kg applied load and 0.5 m/s sliding velocity at 3000 m sliding distances (a) worn surface (b) crack surface. Worn surface topographies of the investigated compacts indicate that the dominant wear mechanism was plowing. The degree of surface damage (i.e. depth and width of the grooves) depended on the applied load and microstructure of the material. At the higher load, generally metallic failure is observed as shown in Fig. 12 (a). For observing the mechanistic phenomenon at the higher load, the SEM micrograph was taken at the higher magnification, as shown in Figure 12b. While studying the wear tracks at different loads for a particular velocity (from 2 to 15 Kg) the operating modes changes from oxidative-to oxidative-metallic to metallic as load applied is increased and wear track observes broken oxide film, deep grooves and delamination of surface as evident from Fig. 12 (b). in this SEM micrograph some small crack was found at the oxide surface. With increase the load, the produce cracks within the material by sliding action easily propagate and the form oxidative film at lower load are ruptured as shown in Figure 12b at 15 Kg load and 0.7m/sec sliding velocity.

3.3.3 Effect of sliding velocity

Self-lubricating role of graphite in sliding contact is provided by layered-lattice structure. Namely, graphite is characterized by hexagonal layered structure. The bonds between the parallel layers are relative weak (Vander Waals type). Except that, graphite reacts with gases (such as water vapor) forming strong chemical bonds. The adsorbed water vapor and other gases from environment onto the crystalline edges weaken the interlayer bonding forces. It results in easy shear and transfer of the crystalline platelets on the mating surfaces. Fig. 13 shows the variation of wear rate with sliding velocity at 2 kg load, 3000m running distance. Like all other aluminum alloys/ composites, Al-Sn/graphite composites also show an initial decrease in wear rate followed by a sharp increase in wear rate after attaining minima with increase of sliding velocity for all composites at different loads. But in all the cases wear rate decreases with increase in graphite content for (say up to 3.4 %graphite in the matrix) all combinations of loads and sliding velocities used.

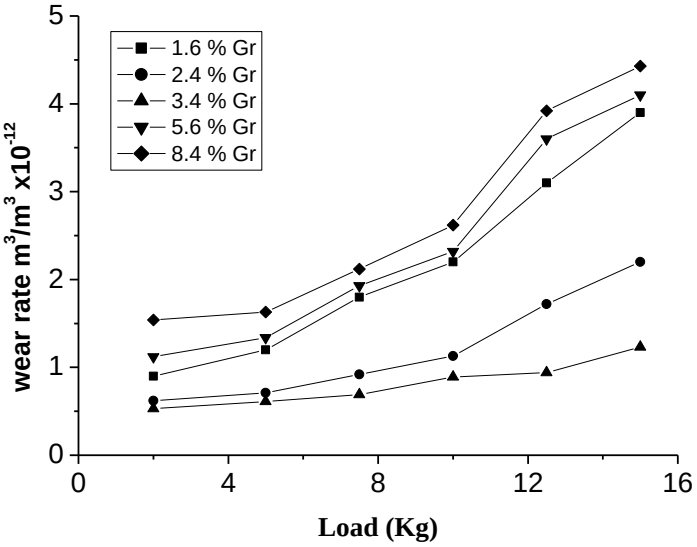

Fig 8. Variation of wear rate with load at 0.5 m/s sliding velocity and running distance 3000 m for as-cast Al-Sn/graphite composites.

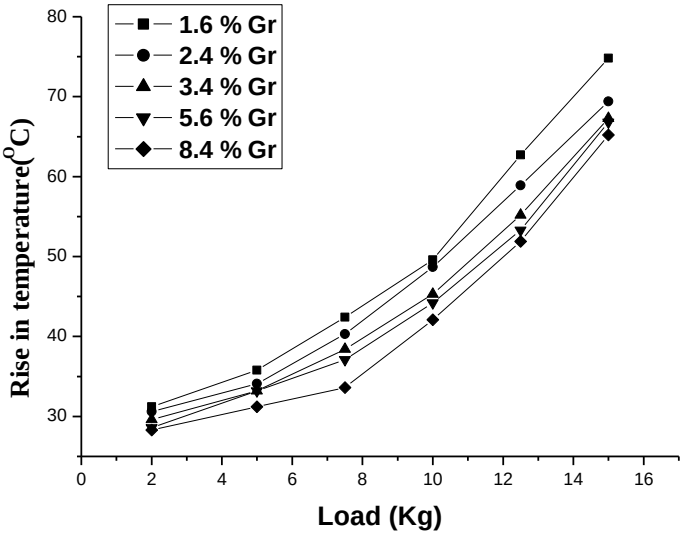

Fig 9. Variation of rise in temperature of the test specimen with load at 3000 running distance and 0.5 m/s sliding velocity for as-cast Al-Sn/graphite composites.

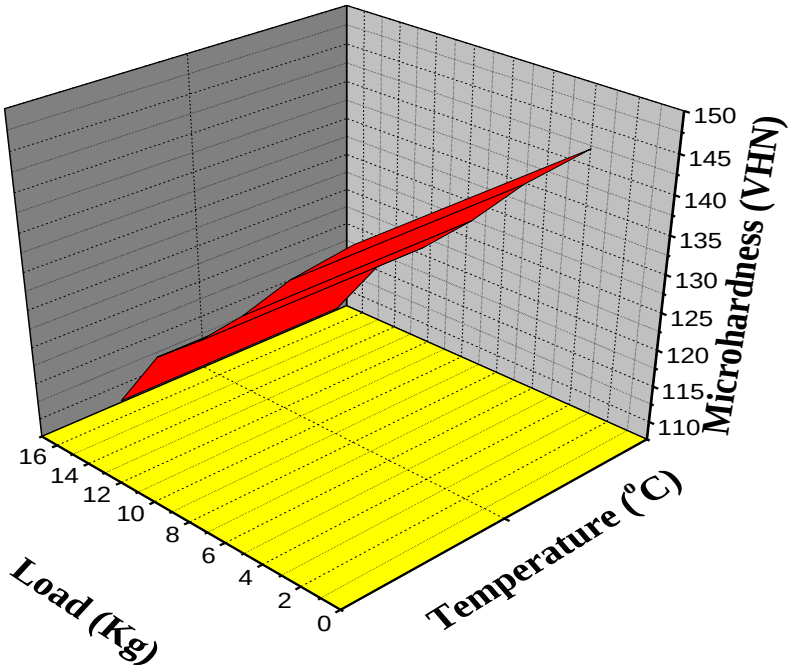

Fig 10. Variation of rise in temperature & micro hardness of the test specimen with load at 3000 running distance and 0.5 m/s sliding velocity for as-cast Al-Sn/graphite composites.

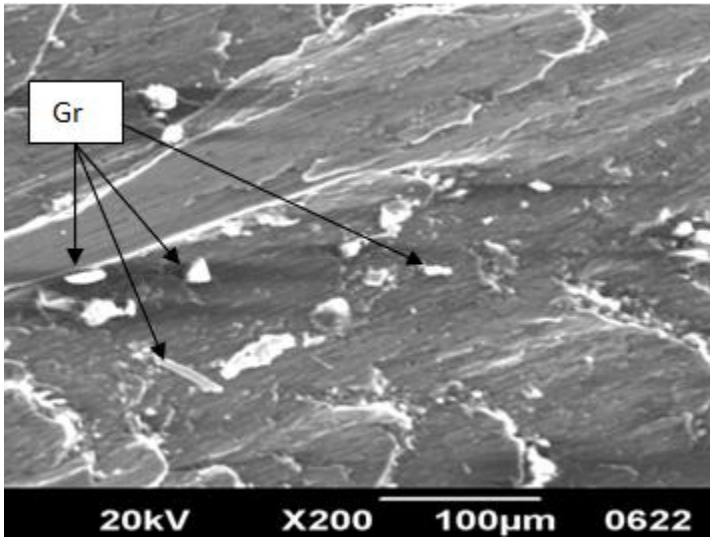

Fig 11. SEM micrographs of wear tracks of Al-Sn/graphite composites (Al-6.3%Sn-3.4%Gr) for 2 kg applied load and 0.5 m/s sliding velocity at 3000 m sliding distances.

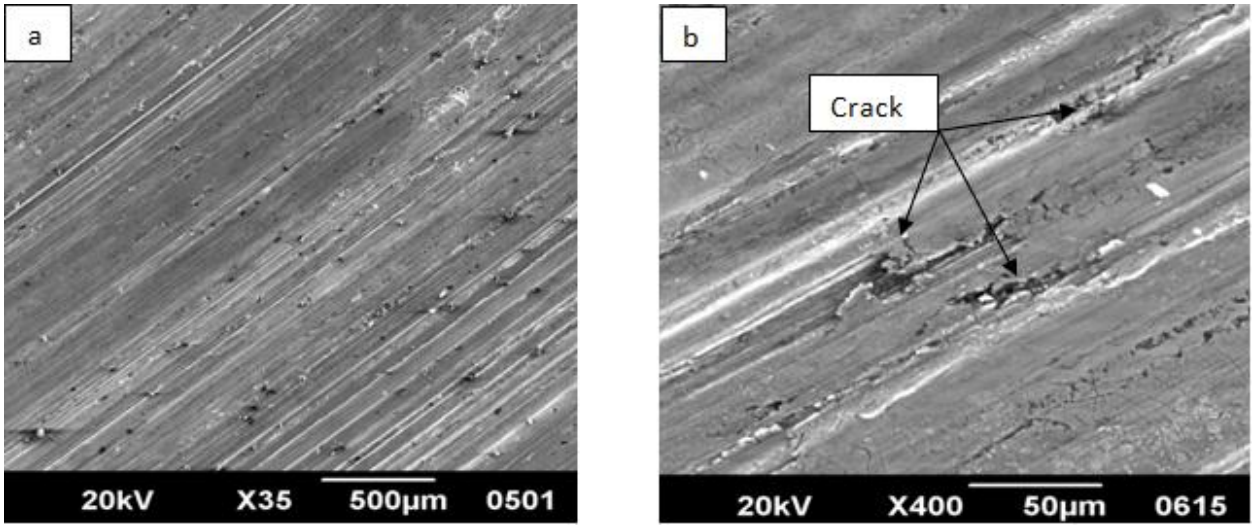

Fig 12. SEM micrographs of wear tracks of Al-Sn/graphite composites (Al-6.3%Sn-3.4%Gr) for 15 kg applied load and 0.5 m/s sliding velocity at 3000 m sliding distances (a) worn surface (b) crack surface

While that wear rate again increase with increase the graphite content in the matrix. Further, variation of wear rate and hardness of worn wear track surface is shown in Fig. 14. It clearly shows highest hardness at minima in wear rate, which is clearly indicative of the presence of hard oxide particles. With increase in sliding velocity, oxides particles are removed from the mating surface, due to decrease the hardness of the composite materials and hence increases the wear rate. Fig. 15 for temperature increase with sliding velocity follows the same trend as observed in the case of variation of temperature with applied load. Higher velocity gives higher amount of wear loss due to fast rubbing of the contacting surface. Therefore maximum rise in temperature in the test specimen at the contacting surface occurs. The SEM observations of the wear tracks at 2.0 Kg load for different sliding velocities are shown in Fig.16 (a–b) and 17(a–c). In Fig. 16 (a-b) shows the SEM observation at the lower and the higher velocity and Fig. 17(a-c) show SEM result at the optimized velocity. SEM micrograph of the wear track in Fig. 16(a) was mainly comprised of oxide particles and the wear track surface is seen to have more pronounced layer of oxide particles adhered at the surface of the materials. But at the higher velocity, metallic particles come out during wear processes and wear tack is seen clear and smooth as shown in Fig. 16(b). The minima in the wear rate was found at 1.22 m/sec. Fig. 17 show SEM micrographs of wear tracks of Al-Sn/graphite composites (Al-6.3%Sn-3.4%Gr) for 2 kg applied load and 1.22 m/s sliding velocity at 3000 m sliding distances (a) worn surface (b) crack observation (c) observation of the oxide layer. Wear rate continuously decreases with increase the sliding velocity due to formation of thin film of oxide layers along with metallic layer at the mating surface as shown in Fig. 17(a). This is confirmed from the SEM observation of the wear track taken at the higher magnification as shown in Fig. 17(b). The oxide layer of the respective metals adhered on the mating surface is clearly visible in this micrograph. The failure of the materials from the wear process is due to formation and propagation of the crack within the materials as shown in Fig. 17(c). The cracks are formed at the adjacent surface of the materials. An examination of the three micrographs shows the formation of severe patches and grooves resulting from plastic deformation of the aluminum graphite composite and relatively small groves and mild patches on 3.4 wt % graphite composite. This reduction in severity of the worn surface of the composite material is due to the formation of a Graphite lubricating film which prevents the direct contact of the specimen with the rotating steel disc surface. This formation of the lubricating layer at the sliding surface becomes thicker with more graphite as the addition of graphite content to the base alloy increases and it is this graphite lubricating layer that is responsible for playing an effective role for keeping the wear behavior of the composite low.

3.4 Study of the surface particles and its mechanistic approach

Fig. 18 a-b shows the SEM micrograph of wear debris for 2 kg applied load and 1.22 m/s sliding velocity at 3000 m sliding distances (a) collecting particles (b) examination of the graphite particles. This observation has been also confirmed by XRD observation as shown in Fig. 19. Debris in all figures

was mainly comprised of oxide particles of aluminum and tin. But it also be contained some small amount of graphite as shown in Fig. 18 b. In the XRD observation, the aluminum oxide, tin and its oxides (from EDAX observation) and graphite are found as the main peak. Tin and lead are weak and ductile and hence they decrease the strength property of aluminum alloys under study. Further, Sn/Pb, being a ductile material, deforms in preference to the stronger matrix. This reduces the stress concentration in the matrix and makes it more deformable. It is also found that the alloys containing tin have slightly more strength and hardness but low ductility values compared to the alloys containing lead. Al wear particles on the worn surfaces are laminated by the pin on the contact area, forming plough. Because wear particles contain some aluminum oxide, Zhou et al believed that the oxidation wear was the main wear mechanism of composites **[24**].However, according to the SEM observation of worn surfaces of the composite and the study of delamination theory of wear, it can be concluded that the delamination wear could be the main wear mechanism. Dislocations at the mating surface, subsurface crack and void are induced due to the repeated plastic deformation between the test pin and disc. The cracks extend later and cause break and split of the hardened surface layer by shear deformation mechanism [**25**].

4. Friction studies

The characterization of friction behaviour of Al-Sn/graphite base composite with sliding at the specific load (i.e. 10N) is illustrated in Fig. 20. The Figure show is graphically representation of the results obtained from the friction experiment at a fixed load and sliding velocity. It is evident from the Fig. 20 the friction coefficient drastically decreases during the running in period. During the steady state period the friction coefficient is being stabilized. In dry sliding, the reason for decreasing the wear rate and the coefficient of friction of Al-Sn/graphite composite as compared with the base alloy is the presence of smeared graphite layer at the sliding surface which acts as the best solid lubricant. The friction behaviour also varies with applied load. The average value of the friction coefficient at normal load is shown in Fig. 21.

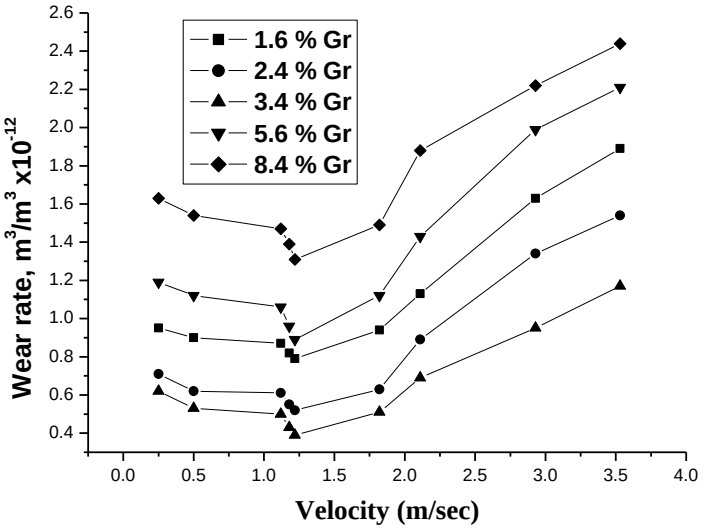

Fig 13. Variation of wear rate with sliding velocity at 2 kg load for Al-Sn/graphite composites.

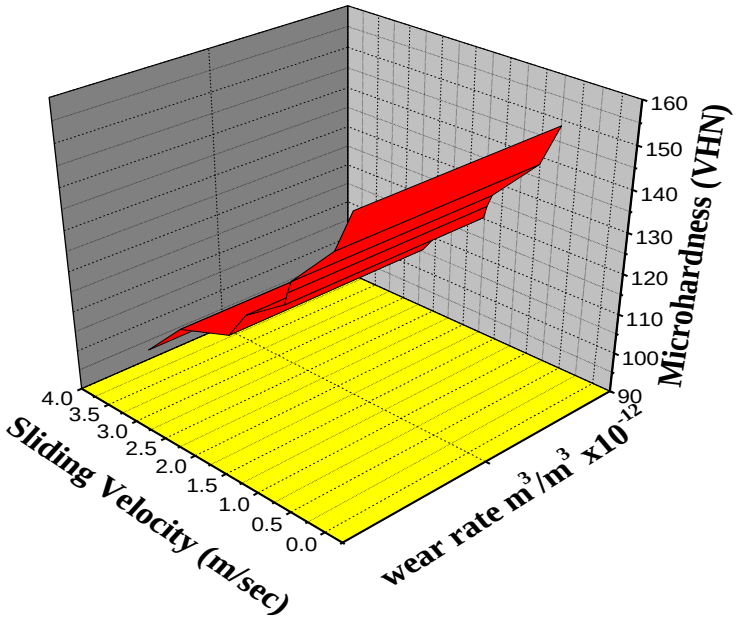

Fig 14. Variation of micro-hardness and wear rate of worn surface with sliding velocity at 2 kg load.

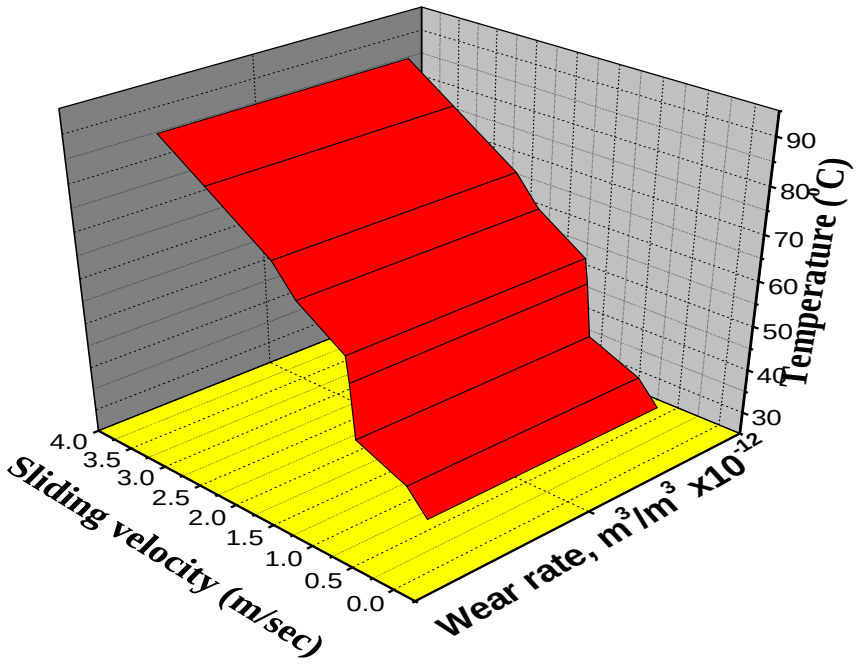

Fig 15. Variation of micro-hardness and wear rate of worn surface with sliding velocity at 2 kg load.

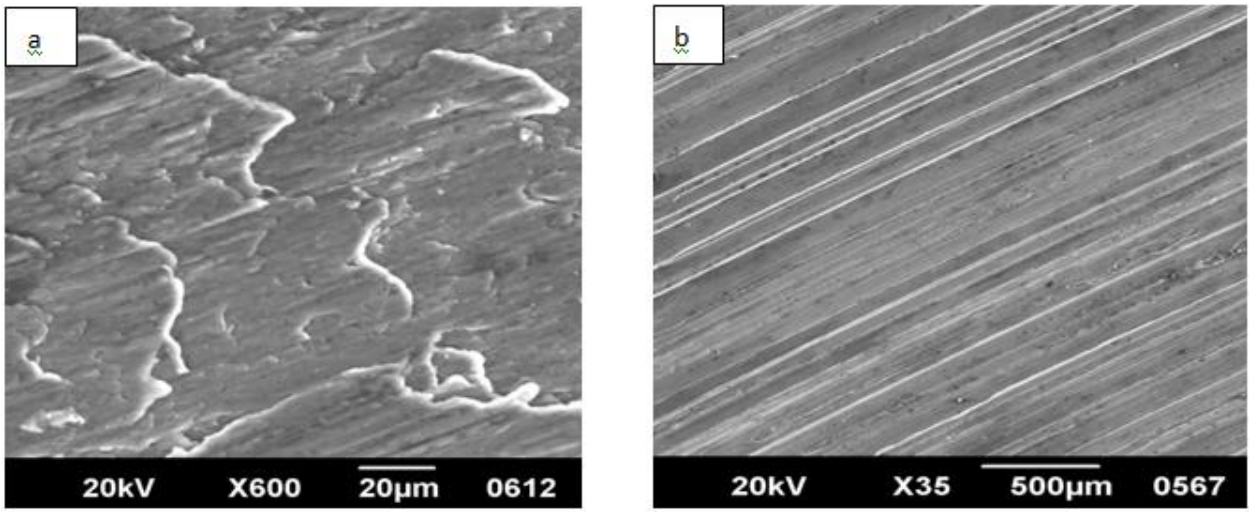

Fig 16. SEM micrographs of wear tracks of Al-Sn/graphite composites (**Al-6.3%Sn-3.4%Gr)** for 2 kg applied load and 0.5 m/s sliding velocity at 3000 m sliding distances (a) worn surface at 0.25m/sec (b) worn surface at 3.53m/sec

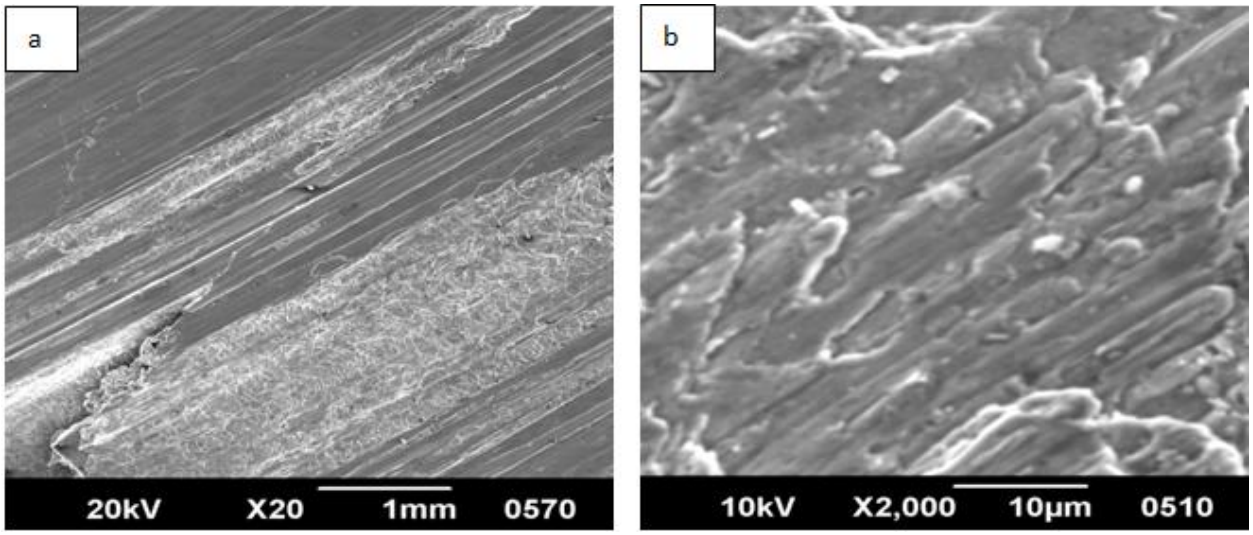

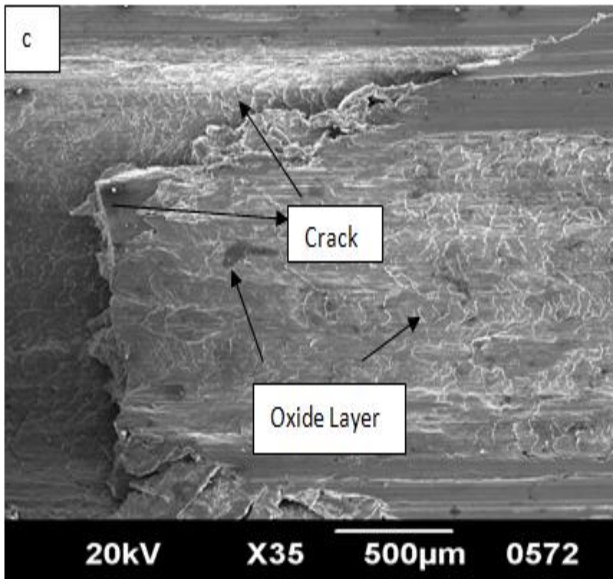

Fig 17. SEM micrographs of wear tracks of Al-Sn/graphite composites (Al-6.3%Sn-3.4%Gr) for 2 kg applied load and 1.22 m/s sliding velocity at 3000 m sliding distances (a) worn surface (b) observation of the oxide layer (c) Crack propagation in oxide layer

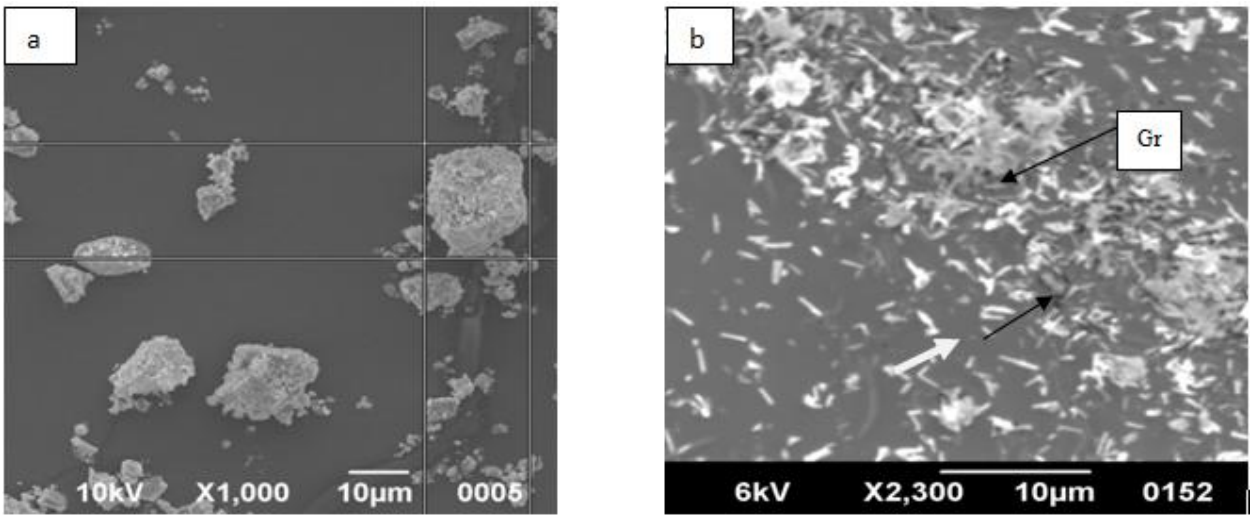

Fig 18. SEM micrographs of wear debris of Al-Sn/graphite composites (Al-6.3%Sn-3.4%Gr) for 2 kg applied load and 1.22 m/s sliding velocity at 3000 m sliding distances (a) collecting particles (b) examination of the graphite particles. In Fig 18(a) X=17.0µm, Y=21.6µm and D=27.5µm

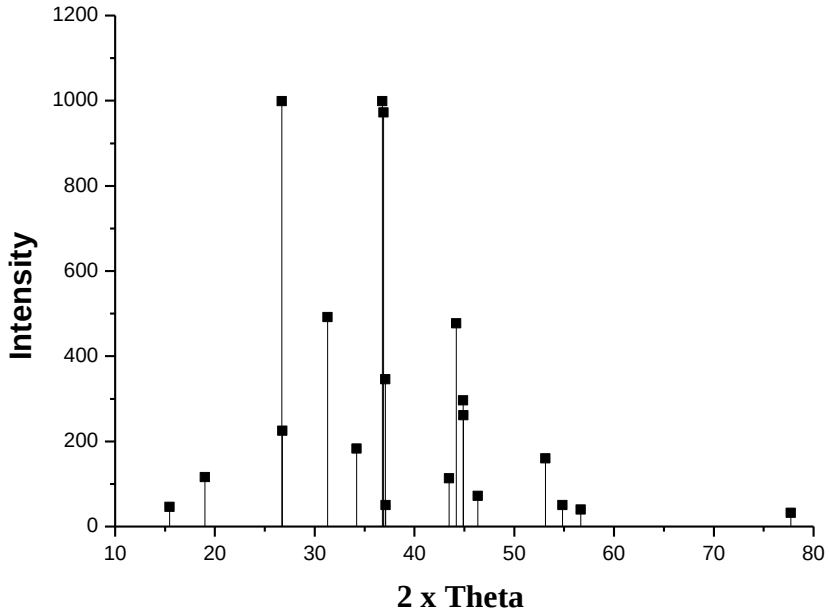

Fig 19. XRD of the wear debris.

In accordance with the figure the increase of the friction coefficient corresponds to increase the normal load. The increase rate is especially evident for load change from 10 to 50 kg. On increasing the applied load, lubricating condition of the graphite deteriorates; the alloy composition starts to play its role in determining the running ability of the test under friction. Fig. 22 shows the variation of coefficient of friction with wt % of graphite content in the matrix. The friction coefficient of the test materials decreases with increase the graphite content in the matrix. With increasing the graphite content, the thickness of the lubricating film and the amount the graphite in the lubricating film increases. The graphite comes more and more contact with sliding surface and results in lowering the frictional coefficients of the composite materials. The worn surfaces of the samples from the SEM examination are shown in Fig. 23. The worn surfaces of the (Al-6.3%Sn-3.4%Gr) samples were noticed to be smoother than those of the (Al-6.3%Sn-8.4%Gr).Generally, the parallel ploughing grooves and scratches can be seen over all the surfaces in the direction of sliding. These grooves and scratches resulted from the ploughing action of asperities on the counter disc of significantly higher hardness. The worn surfaces of the samples from the SEM examination are shown in Figure 23 a-b. The worn surfaces of the test sample were noticed to be smoother at the higher load than at the lower load as shown in Fig 23. Generally, the parallel ploughing grooves and scratches can be seen over all the surfaces in the direction of sliding. These grooves and scratches resulted from the ploughing action of asperities on the counter disc of significantly higher hardness.

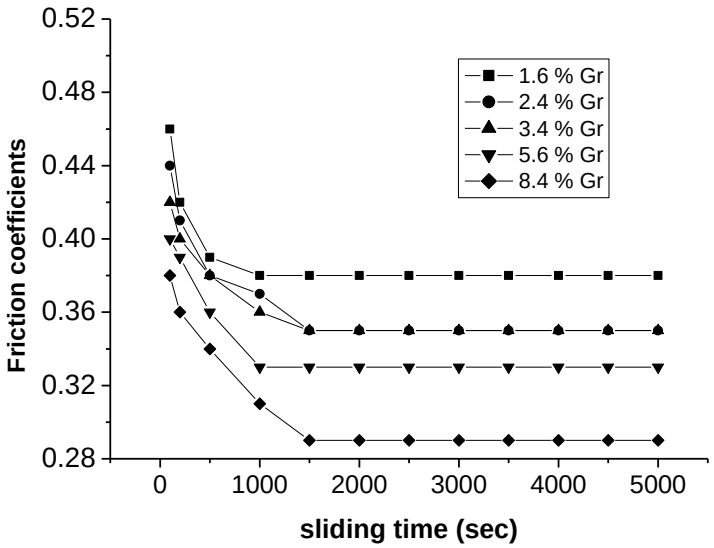

Fig 20**.** Friction coefficient variation of (Al-Sn/Gr) composite during sliding time at fixed specific loads (i.e. 10N) and sliding speeds (1.22 m/sec)

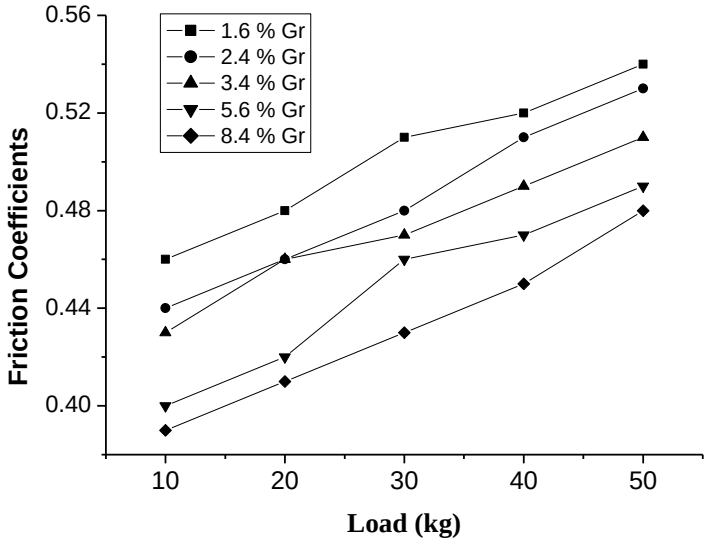

Fig 21**.** Coefficient of friction vs. applied load for (Al-Sn/Gr) composite at 0.932m/sec

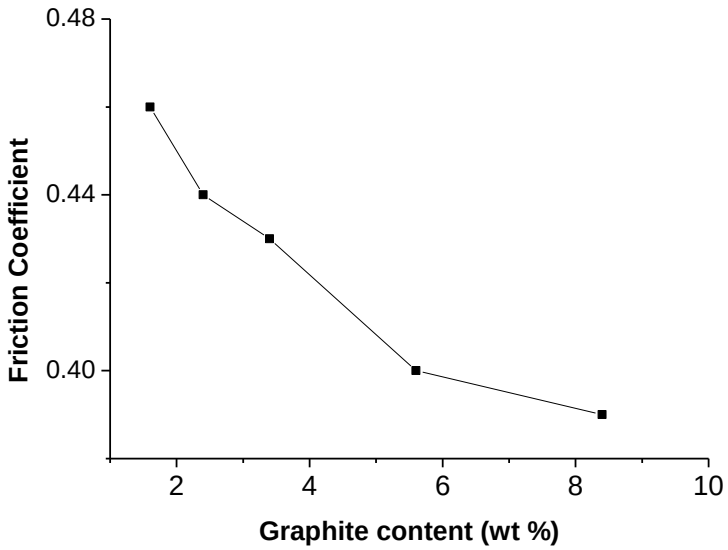

Fig 22. variations in the coefficient of friction with the wt % of graphite in the matrix.

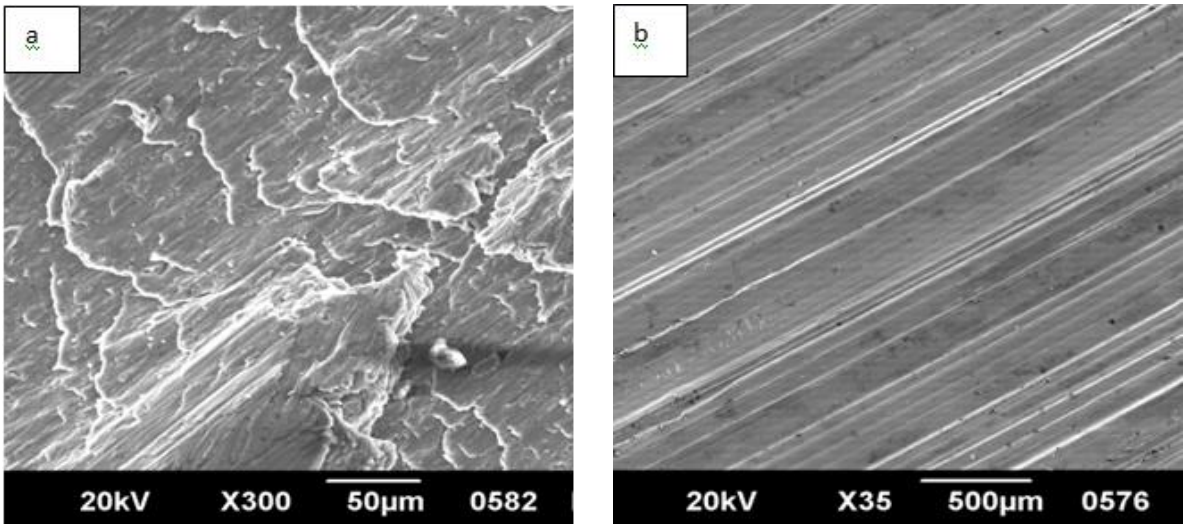

Fig 23. SEM micrographs of wear debris of Al-Sn/graphite composites (Al-6.3%Sn-3.4%Gr) for 2 kg applied load and 1.22 m/s sliding velocity at 3000 m sliding distances (a) at lower loads (b) at higher loads.

5. Conclusion

1. The Al-Sn/Graphite composite is being prepared from liquid metallurgical methods. It can be observed from the present investigation that graphite could be successfully and uniformly distributed in aluminium-tin base matrix using impeller mixing chill casting technique.
2. UTS, 0.2%PS and VHN increased with decreases with increases the volume fraction of the graphite in the matrix.
3. The Al-6.3%Sn-8.4%Gr composite showed higher percentage of elongation while compared to Al-6.3%Sn-1.6%Gr
4. From the present investigation we have also observed that the ductility of composite increase with increase the percentage of graphite.
5. The hardness is another affecting parameter which affects the rate of wear, decreases with increase the percentage of graphite in the matrix.
6. At higher contents, a graphite agglomeration is presented, and this effect reduces the mechanical resistance. This variation is related to the graphite dispersion / agglomeration into aluminum alloy matrix.

7. Wear rate with sliding distance shows almost a linear relationship for all combinations of loads and sliding velocities and composites.
8. Wear rate increases continuously with applied load for all the sliding velocities and composites studied.
9. Wear rate initially decreases with increase in sliding velocity attains a minima in wear rate and then increases with further increase in sliding velocity for all the loads and composites.
10. Low loads and sliding velocities are dominated by oxidative debris whereas higher loads and sliding velocities are dominated by metallic debris..
11. At low loads and sliding velocities wear track surface is largely covered with oxide layer and smooth in nature but at higher loads or sliding velocities surface is highly deformed with deep grooves and gross delamination occurs leading to larger wear rate.
12. The coefficient of friction decreases with increase the graphite content in the matrix.

Reference

[1] **A. N**. **Patel** and **S Diamond**., Mater. Sci. Eng. **98**, 329 (1988).
[2] **J. P**. **Pathak**, **V Singh**., and **S. N. Tiwari**, J. Mater. Sci. Lett. **11**, 639 (1992).
[3] **T. B. Massalki**, *Binary Alloy Phase Diagrams* (American Society for Metals, Metals Park, OH, 1986).
[4] **L. Ratke**, and **S. Diefenbach**, Mat. Sci. Eng. **R15**, 263 (1995).
[5] **R. N. Singh** and **F. Sommer**, Rep. Prog. Phys. **60**, 57 (1997).
[6] **L. F**. **Mandolfo**, Aluminum Alloys, structure and properties, Butterworth's London (1976), 8585
[7] **A.K. Jha**, **S.V Prasad**., **G.S**. **Upadhyaya**, Dry sliding wear of sintered 6061 aluminium alloy / graphite particle composite, Tribology International, (1989) p 321-327.
[8] **A.K**. **Jha**, **S.V**. **Prasad**, **G.S. Upadhyaya**, Sintered 6061 aluminium alloy – Solid lubricant particle composites: Sliding wear and Mechanism of lubrication, Wear 133 (1989) p 163-172.
[9] **R.C Prasad.,** and **P**. **Ramakrishnan** Composites Science & Technology, New Age International Publishers, (2009).
[10] **F. Akhlaghi,** and **A. Zare-Bidaki,** Influence of graphite content on the dry sliding and oil impregnated sliding wear behavior of aluminium 2024 – graphite composites produced by in situ powder metallurgy method. Wear 266 (2009) 37-45.
[11] **P.K**. **Rohatgi** and **B.C**. **Pai**, Seizure Resistance of Cast Aluminum Alloys Containing Dispersed Graphite Particles of Various Sizes, Wear, 1980, 59, p 323–332
[12] **S.V Prasad.** and **R Asthana**., Aluminum Metal Matrix Composites for Automotive Applications: Tribological Considerations, Tribol. Lett., 2004, 17(3), p 445–453
[13] **P.R Gibson**., **A. J Clegg**. and **A.A. Das**, Mater. Sci. Technol. 1 (1985), p 559-567.
[14] **P.R Gibson**., **A. J Clegg**. and **A.A. Das**, Wear of cast Al-Si alloys containing graphite: Wear, vol 95(1984) p193-198.
[15] **S. Das**, **S.V. Prasad**, **T.R. Ramachandran**, Wear 133 (1989) p 173-187.
[16] **C.B. Lin, R.J. Chang, W.P. Weng**., A study on process and Tribological behavior of aluminum alloy / Graphite particle composite, Wear 217 (1998), p 167-174.
[17] **T. Savaskan, and A**. **Aydiner** Effects of silicon content on the mechanical and tribological properties of monotectoid-based zinc-silicon-silicon alloys, Wear 257(2004) ,p 377-388,.
[18] **B. K Prasad** Effects of microstructure on the sliding wear performance of Zn-Al-Ni alloy, Wear 240(2000), p100-112.
[19] **G. Purcek, T. Kucukomeroglu, T. Savaskan.,** and **S. Murphy**.: Dry sliding friction and wear properties of zinc-based alloy, Wear 252(2002), p 894 – 901,
[20] **S. Mohan**. and **S. Srivastava** Surface behaviour of as-Cast Al–Fe intermetallic composites. Tribology Letters, Vol. 22, No. 1, April (2006).
[21] **B.S. Majumdar, A.H. Yegneswaran,** and **P.K. Rohatgi,** Strength and Fracture Behavior of Metal Matrix Particulate Composites, Mater. Sci. Eng., (1984), 68, p 85–96
[22] **K.K Chawla**., Composite Materials, 2nd ed., Springer, New York, 1998, p 3–5
[23] **T.W Clyne**. and **P.J .Withers.,** An Introduction to Metal Matrix Composites, 1st ed., Cambridge University Press, Cambridge, (1993), p 1–10.
[24] **Sheng-ming Zhou, Xiao-bin Zhang, Zhi-peng Ding, Chun-yan Min, Guo-liang Xu, Wen-ming Zhu.** Fabrication and tribological properties of carbon nanotubes reinforced Al composites prepared by pressureless infiltration technique [J]. Composites Part A: Applied Science and Manufacturing, (2007), 38(2): 301−306.
[25] **N. P. Suh** The delamination theory of wear [J]. Wear, (1973), 25(1): 111−124.−13